Ecological Informatics 91 (2025) 103410

Contents lists available at ScienceDirect

Ecological Informatics

journal homepage: www.elsevier.com/locate/ecolinf

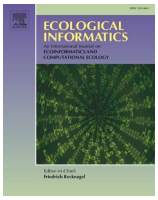

Assessment of pollutants from the Canale d'Aiedda basin to the sea: SWAT model and Remote Sensing Approach

Marco Centanni [a], Rose Mary [a], Giovanni Romano [a], Giovanni Francesco Ricci [a,*], Ossama M.M. Abdelwahab [a], Julio Pérez-Sánchez [c], Anna Maria De Girolamo [b], Francesco Gentile [a]

[a] Department of Soil, Plants and Food Sciences, University of Bari Aldo Moro, Bari, Italy
[b] National Research Council, Water Research Institute, Bari, Italy
[c] Universidad de Las Palmas de Gran Canaria, Gran Canaria, Spain

ARTICLE INFO

Keywords:
SWAT model
Sentinel-2
Sediment load
Nutrient transport
Plume deposition
Intermittent River

ABSTRACT

Water quality impairment is a concern in water resources management. During floods, a large amount of sediment and pollutants may be delivered to the river reaching the coastal zone and forming plumes that impact coastal water bodies. The present paper aims to assess spatial patterns of pollutants from the catchment to the sea, identifying the sources of nutrients within a basin, and their fate in the sea. An ecohydrological model, Soil & Water Assessment Tool (SWAT), and remote sensing techniques (Sentinel-2 imagery, processed on Google Earth Engine), using the Normalized Difference Turbidity Index (NDTI), were coupled and tested in the Canale d'Aiedda basin and Mar Piccolo Sea (Apulia, Southern Italy). The SWAT model was calibrated using daily flow and discrete sediment and nutrient concentrations. The highest specific load of total nitrogen (TN) (~10 kg $ha^{-1}y^{-1}$) was simulated in the agricultural subbasins (vineyards, olive groves, and winter wheat). Similarly, the highest specific load of total phosphorus (TP) (0.7 kg $ha^{-1}y^{-1}$) was predicted in the subbasins where the vineyard was the prevalent crop production. NDTI was analyzed for detecting sediment concentrations in river plumes during a flash flood event (0.066 m^3s^{-1}, June 10, 2023). The post-event NDTI showed increased turbidity along the coast. The results indicate that flash floods play an important role in sediment and pollutant loads delivered to the sea. This study also shows that Sentinel-2 satellite data and cloud computing enhanced turbidity monitoring into the sea or lake, complementing the SWAT results. The methodology applied in the study showed that hydrological models and remote sensing should be coupled for basins and coastal areas ecosystems protection.

1. Introduction

Water quality deterioration represents one of the most pressing environmental challenges of the 21st century, with significant implications for ecosystem health, human well-being, and economic sustainability (Reid et al., 2019; Vörösmarty et al., 2010). Anthropogenic activities have dramatically altered the hydrological cycle and nutrient fluxes, leading to widespread degradation of freshwater and marine ecosystems globally (Grizzetti et al., 2019; Steffen et al., 2020). Despite substantial policy interventions, including the European Water Framework Directive and Marine Strategy Framework Directive, recent assessments indicate that only 40 % of European surface waters achieve good ecological status (European Space Agency(ESA), 2015; Carvalho-Santos et al., 2016).

Sustainable watershed management is an important goal for the communities, especially in the Mediterranean Region, where water resources are limited. In this Region, intermittent rivers are predominant and constitute an important source of water for both human activities and ecological features (Tramblay et al., 2021a, 2021b). Several studies reported that both diffuse and point sources may be critical pressures for intermittent and ephemeral streams (Magand et al., 2020; Ricci et al., 2022). For these river systems, flash floods assume a key role in sediment and nutrient export to the stream (Fouilland et al., 2012). Significant amounts of sediments and pollutants are mobilized from terrestrial sources and transported to the sea during floods, forming plumes that may impact coastal water bodies and influence coastal water properties and circulation (Horner-Devine et al., 2015; Mallin et al., 2016; Osadchiev and Korshenko, 2017; Sauvage et al., 2018).

* Corresponding author at: Department of Soil, Plants and Food Sciences, University of Bari Aldo Moro, Via Amendola 165/A, Bari 70126, Italy.
E-mail address: giovanni.ricci@uniba.it (G.F. Ricci).

https://doi.org/10.1016/j.ecoinf.2025.103410
Received 20 June 2025; Received in revised form 31 July 2025; Accepted 26 August 2025
Available online 4 September 2025

Sediment loads transported by rivers constitute both natural geomorphological processes and anthropogenically enhanced phenomena with significant ecological implications (Wohl et al., 2019; Yang et al., 2017). Excessive sediment delivery to coastal environments can lead to habitat smothering, reduced light penetration, and altered benthic community composition (Delgado-Fernandez et al., 2019; Schaeffer et al., 2015). Furthermore, sediments often serve as vectors for contaminants, including heavy metals and organic pollutants (González-Ortegón et al., 2019; Liu et al., 2007). Understanding the source of pollutants, their spatial and temporal variability, and the plume dynamics is crucial for assessing the potential impacts on water quality and identifying watershed and coastal management strategies (Álvarez-Romero et al., 2013; Devlin et al., 2015).

Integrated river basin management employs several methodological approaches. Ecohydrological modeling has gained significant traction in recent decades (Centanni et al., 2024; da Burigato Costa et al., 2019; Malagó et al., 2019), offering robust capabilities for quantifying sediment and pollutant transport to marine environments while identifying critical source areas within watersheds. The Soil and Water Assessment Tool (SWAT) has emerged as a powerful ecohydrological modeling framework for quantifying sediment and nutrient transport processes across diverse spatial and temporal scales (Arnold et al., 1998; Ricci et al., 2022). Concurrently, advancements in satellite sensors have substantially enhanced the applicability of remote sensing techniques in water quality assessment and coastal dynamics (Álvarez-Romero et al., 2013; Devlin et al., 2015; Gancheva et al., 2021; Lega and Endreny, 2016; Petus et al., 2014; Zablan et al., 2023). Satellite-derived optical indices, particularly those leveraging multispectral sensors such as Sentinel-2 and Landsat-8, provide powerful tools for delineating plume extent, turbidity gradients, and sediment deposition patterns (Cabezas-Rabadán et al., 2019; Kastridis et al., 2020; Lega and Endreny, 2016). Process-based models, coupled with remote sensing data, may support decision-making for water resource management in Mediterranean water systems (Álvarez-Romero et al., 2013; Kaplan et al., 2024; Le Page et al., 2020; Li et al., 2014).

Despite the technological advances, significant knowledge gaps persist regarding the fate and transport of sediments and associated pollutants across the land-sea interface, particularly in regions characterized by intermittent streams (Borg Galea et al., 2019; Skoulikidis et al., 2017) characterized by flashy hydrographs, high erosion rates, and complex hydrological behaviors (Fortesa et al., 2021; Nerantzaki et al., 2015). While extensive research exists on large perennial river plumes (Dagg et al., 2004; Horner-Devine et al., 2015; Mendes et al., 2016; Osadchiev and Korshenko, 2017), smaller episodic watersheds remain understudied (Joumar et al., 2023). Furthermore, integrated approaches that couple watershed-scale process modeling with remote sensing of coastal plumes remain underrepresented in the scientific literature.

This study addresses these research gaps by developing and implementing an integrated methodological framework that combines SWAT modeling with satellite-derived turbidity indices to characterize the complete source-to-sea continuum of sediment and nutrient transport in a Mediterranean watershed. Specifically, this research aims to: (1) quantify spatial and temporal patterns of sediment and nutrient generation within the Canale d'Aiedda basin; (2) identify critical source areas contributing disproportionately to pollutant loading; and (3) characterize the extent, intensity, and deposition patterns of sediment plumes in the receiving Mar Piccolo coastal embayment during a flash flood event. By integrating terrestrial watershed modeling with coastal remote sensing observations, this study provides a novel methodological framework applicable to similar watersheds globally, while generating actionable information to support integrated coastal zone management in the study region.

2. Materials and methods

2.1. Study area

Canale d'Aiedda is a watershed (Fig. 1) located in the Puglia Region in Southern Italy. The Mediterranean region's representative climate, land cover, and management practices are exemplified in this 360 km^2 basin, which drains into the Mar Piccolo's second inlet, an inner semi-enclosed sea (D'Ambrosio et al., 2019).

Agriculture is the main anthropogenic activity in the basin. Vineyards, olive trees, almond trees, orange groves, vegetables, and arable land are the most widespread land uses and cover almost 88 % of the total area. Urban areas are of medium size and occupy 4 % of the total basin area (D'Ambrosio et al., 2020). Soils range from clayey silt to sandy loam (D'Ambrosio et al., 2019). Three wastewater treatment plants (WWTPs), located in the municipalities of Montemesola, Monteiasi, and San Giorgio Ionico, discharge treated wastewater into the river system. The stream feeds a protected area (WWF oasis, 1.16 km^2), "Palude la Vela" wetland, which is part of the Site of Community Importance "Mar Piccolo" (IT9130004). This wetland is an important site for various residents (i.e., grey herons and finches), and migratory birds (i.e. flamingos and curlews). The stream shows an intermittent character; it is mainly characterized by concrete beds and banks. The river is dry for most of the year, whereas the river segments downstream of the WWTPs are perennial (Ricci et al., 2022).

The Mar Piccolo is characterized by a long tradition of activities related to mussel farming, especially in the second inlet, with an annual production ranging from 7000 and 8500 t (Petrosillo et al., 2023). The surrounding area has been influenced by industrial development, which has brought economic growth and environmental implications. From a naturalistic point of view, Mar Piccolo stands out for its conformation and the presence of a rich ecosystem. The biodiversity is also linked to the presence of submarine springs at the bottom of the marine basin (Zuffianò et al., 2016), called "citri", which contribute to influencing ecosystems and water quality.

Given the ecological importance of the Mar Piccolo's biodiversity, it is essential to conduct studies that assess the potential release of contaminants from surrounding drainage areas and identify appropriate environmental protection and restoration measures. The balance between development and conservation is one of the main challenges for the future of Mar Piccolo, an area that, despite the critical issues, may have a high potential ecological value (Trinchera et al., 2015).

2.2. SWAT model set up and calibration

The SWAT model is a widely utilized semi-physical, spatially distributed hydrological, and water quality model designed for predicting streamflow, sediment, and nutrient loads in both gauged and ungauged river basins (Arnold et al., 1998). SWAT discretizes a basin into sub-basins based on user-defined drainage thresholds and further into hydrological response units (HRUs) according to land use, slope, and soil properties (Neitsch et al., 2011). For this study a threshold of 350 ha was used to obtain 40 subbasins, while thresholds of 10 % of land use, 10 % of soil classes, and 20 % slopes were used to discretize HRUs. Surface runoff can be calculated using either the Soil Conservation Service curve number (SCS-CN) method or the Green-Ampt method, with this study employing the SCS-CN method (Soil Conservation Service (SCS), 1972). Potential evapotranspiration (PET) is estimated using the Penman-Monteith, Priestly-Taylor, or Hargreaves methods, with this work utilizing the Hargreaves method (Hargreaves and Samani, 1985). The sediment yield is estimated by using the Modified Universal Soil Loss Equation (MUSLE) (Williams, 1975). Sediment degradation or deposition in the channel is simulated through a simplified version of Bagnold's stream power relationship (Bagnold, 1977). The nutrient cycle is modeled using a mass balance approach as described by Neitsch et al. (2011) derived from the QUAL2E model (Brown and Barnwell,

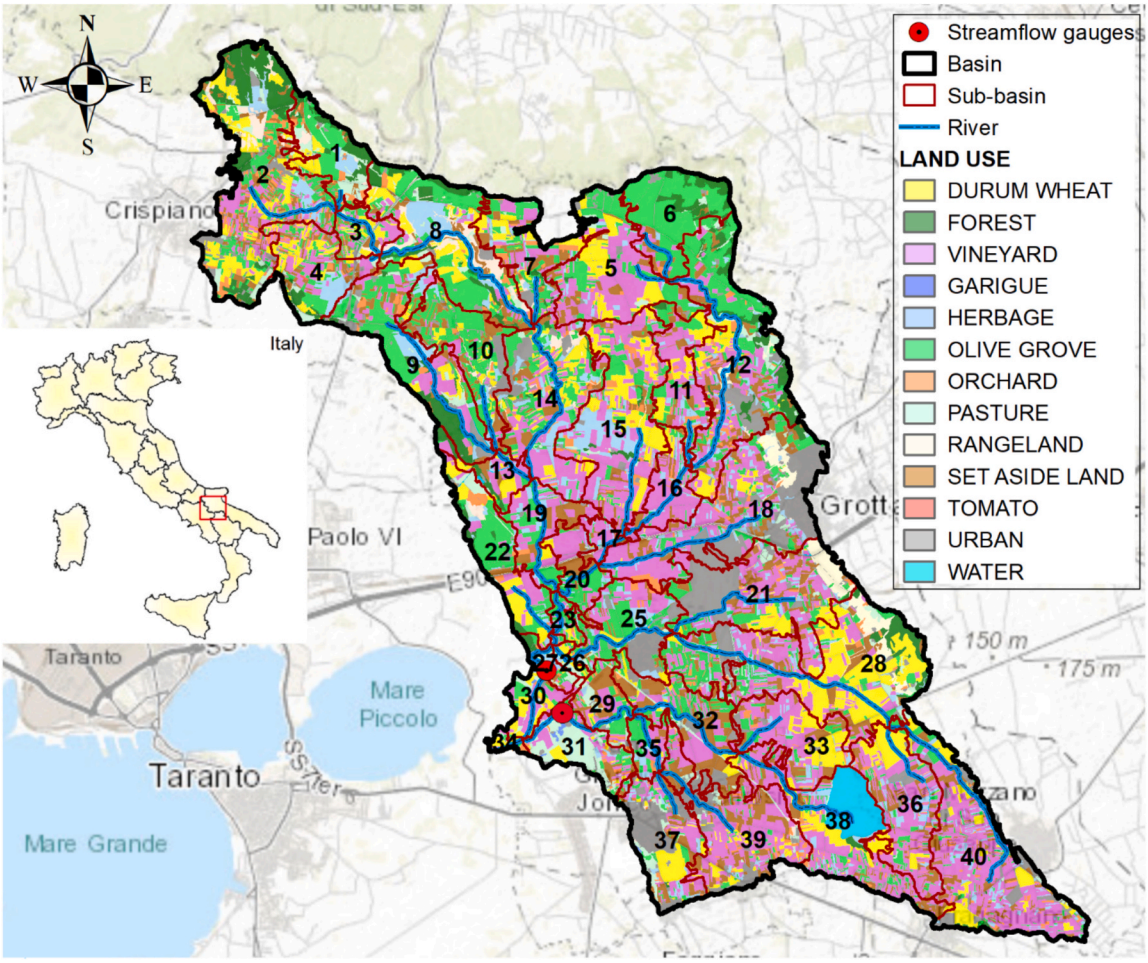

Fig. 1. Study area: Canale d'Aiedda basin. Land use classes and sub-basins.

1987). Spatial data necessary for model setup include Digital Elevation Model (DEM), soil map, and land use map (reclassified using specific SWAT codes) (Table 1).

The study integrated land use and soil data into the SWAT geodatabase, identifying 13 land use classes and 11 soil types (D'Ambrosio et al., 2019). Crop management practices, informed by farmer interviews, were also incorporated. For vineyards, tillage occurred twice at 10 cm depth in February and May, and once at 35 cm depth in October, with fertilizers applied in February and October (types 12–12-17 and 10–5-15) and organic manure in November. Irrigation spanned from May to September, totaling 2400 m^3 ha^{-1} annually. Olive management involved three shallow tillages in April, August, and November, with fertilizer applications in April (urea and 12–8-8) and August (13–46-0), and irrigation from June to September totaling 500 m^3 ha^{-1} annually. Durum wheat, planted in November and harvested in July, had deep tillage in August, shallow tillage in October, and fertilizers applied in December (25–15-0) and February (urea). Minor crops underwent shallow tillage in spring and deep tillage in autumn, and auto-irrigation and auto-fertilization functions were used. The USLE P (Universal Soil Loss Equation – Support practice factor) factor was set to 1 due to the lack of conservation practices. The river basin was divided into 40 sub-basins, with HRUs discretized using thresholds of 10 % for land use, 10 % for soil properties, and 20 % for slopes, generating 271 HRUs. It was verified that the thresholds maintained the original proportion of land use and soil types, excluding only minor classes. SWAT was run from 2014 to 2023 (with three years of warm-up) and calibrated for streamflow, sediment, and nutrients.

Sensitivity analysis and calibration were conducted using the SWAT-Calibration and Uncertainty Programs (SWAT-CUP) tool, employing the Sequential Uncertainty Fitting (SUFI-2) algorithm as described by Abbaspour et al. (2015), to achieve a proper model performance. The parameters included into the sensitivity analysis were selected based on literature and on previous studies carried out in the same study area (Arnold, 2012; D'Ambrosio et al., 2020). Streamflow data, at daily time scale from 2017 to 2021, measured at the two gauging stations, located in subbasins 27 and 29 (Fig. 1) were used for calibrating hydrology. Discrete nutrient concentrations measurement of sediment, total nitrogen (TN) and total phosphorus (TP), collected in the same period (2017–2021), were used to calibrate water quality. The evaluation of model performance was judged based on the following statistical metrics.

Nash & Sutcliffe efficiency (NSE) (Nash and Sutcliffe, 1970)

$$NSE = 1 - \left[\frac{\sum_{i=1}^{n}\left(Y_i^{obs} - Y_i^{sim}\right)^2}{\sum_{i=1}^{n}\left(Y_i^{obs} - Y^{mean}\right)^2}\right] \quad (1)$$

Percent bias (PBIAS)

$$PBIAS = \left[\frac{\sum_{i=1}^{n}\left(Y_i^{obs} - Y_i^{sim}\right)*(100)}{\sum_{i=1}^{n}\left(Y_i^{obs}\right)}\right] \quad (2)$$

Coefficient of determination (R^2)

Table 1
Source and spatial resolution of the input data used for the SWAT model setup.

Input	Source	Resolution
Digital elevation model	Puglia Region (http://www.sit.puglia.it).	8 × 8 m
Land use map	Puglia Region land use map (http://www.sit.puglia.it) integrated by using National Agricultural Census data (dati-censimentoagricoltura.istat.it). Arable land was categorized into durum wheat, set-aside land, and herbage.	1:5000 (21 land uses)
Soil map and database	Puglia Region (2001) ACLA2 project Joint Research Centre European Soil Data Centre (JRC-ESDAC) (https://esdac.jrc.ec.europa.eu/resource-type/datasets	1:100000 500 × 500 m (11 soil types)
Point sources (Waste Water Treatment Plants)	Puglia Water Authority (personal communication) Regional Agency for Environmental Protection (http://www.arpa.puglia.it/web/guest/depuratori) Puglia Region (http://www.sit.puglia.it)	-
Meteorological data	Civil Protection Service – Puglia Region (https://protezionecivile.puglia.it/) Regional Agency for Irrigation and Forestry Activities (http://www.agrometeopuglia.it/	-
Agricultural practices	Farmers' and dealers' interviews (D'Ambrosio et al., 2019) on agricultural practices: tillage operations (type and date), fertilizer and irrigation applications (timing, amount, type). Grazing was considered on pasture.	-

$$R^2 = \left[\frac{\sum_{i=1}^{n}\left(Y_i^{obs} - Y_i^{sim}\right)}{\sum_{i=1}^{n}\left(Y_i^{obs} - Y_i^{mean}\right)}\right] \quad (3)$$

Following the guidelines proposed by Moriasi et al. (2007), the model prediction was considered satisfactory when both NSE and R^2 exceeded 0.5 and PBIAS ranged between −25 % and + 25 %. To evaluate all the different hydrological conditions (wet and dry), it was decided to use all the series for the calibration (Centanni et al., 2024).

2.3. Remote sensing approach for plume detection

2.3.1. Remote sensing data

The remote sensing data used in this study were acquired from Sentinel-2 L2 A satellite images, available on the Google Earth Engine (GEE) platform after online access to a centralized repository of georeferenced and atmospherically corrected satellite multispectral images. The Copernicus Sentinel-2 mission of the European Space Agency (ESA) includes two polar-orbiting satellites, Sentinel-2 A and Sentinel-2B, equipped with advanced high-resolution multispectral imagers (MSI) providing a set of 13 spectral band images from the visible to the shortwave infrared, at 10, 20, and 60 m spatial resolution. The twin satellites ensure a nominal revisit time of five days and a global absolute geolocation accuracy of the images better than 6 m (European Space Agency(ESA), 2015). The Sentinel-2 image collection for the area of interest (AOI) (Mar Piccolo at the mouth of the d'Aiedda stream) was selected and processed via cloud computing. A multiple filter preprocessing step was applied to remove all the images with more than 10 % cloud cover, develop the imagery time series for both the selected period and the region of interest (ROI), intersect the boundaries of AOI, and select the spectral bands to be used for the normalized indices extraction. Rainfall events and floods recorded at the gauging stations were preliminarily identified to filter the time. Despite several images from 2017 to 2023 were considered, due to data availability constraints (i.e. presence of clouds), only images related to the flood event of June 10th 2023 (Figure Annex 1) were suitable to highlight the dispersion of pollutants delivered into the sea. This event was chosen because it coincided with cloud-free satellite overpasses, ensuring optimal observation conditions over the area. Two images were subsequently chosen to investigate the water turbidity levels before and after the flood event, enabling a comparative analysis of its environmental impact.

2.3.2. Spectral indices

Several normalized spectral indices are available in the literature to identify water surface, water quality, suspended sediment, water turbidity, and chlorophyll concentration (Vizzari, 2022; Zablan et al., 2023). This study, focused on extracting water surface and detecting water turbidity parameters using the indices shown in Table 2.

Starting from Sentinel-2 imagery, two of the most widely used indices to distinguish water surfaces from dry land automatically were applied: the Automated Water Extraction Index (AWEI) and the Normalized Difference Water Index (NDWI). Given the absence of clouds, reliefs, and building shadows, the results achieved by both indices had high accuracy and similar responses (Figure Annex 2; Figure Annex 3). NDWI seems more accurate only in the Southeastern part of the area (Fig. 2), then water extraction was performed using such index and selecting a threshold value (0.07) from the NDWI frequency distribution.

Water turbidity was assessed using Normalized Difference Turbidity Index (NDTI), specifically developed by Lacaux et al. (2007) to calculate this water parameter from remote sensing data. NDTI operates on the assumption that an increase in turbidity will result in higher reflectance in the red band compared to the green band.

3. Results

3.1. SWAT model performance and calibration analysis

The study identified many hydrological and water quality parameters that significantly influence streamflow, sediment, and nutrient concentrations (Table 3). Specifically, the Curve Number (CN2) and the parameters related to evapotranspiration, transmission losses, and infiltration to aquifers were the most sensitive for hydrological processes. The calibration results for streamflow were satisfactory for gauge A and good for gauge B (Figure Annex 4a, Fig. 4b; Table 4). The statistical performance metrics were R^2 0.60, NSE 0.58, PBIAS +23.00 for gauge B (Reach 27) and R^2 0.50, NSE 0.50, PBIAS 0.00 for gauge A (Reach 29).

During the calibration period, observed daily mean flow at gauge A was 0.034 m^3s^{-1}, ranging from 0.006 to 0.548 m^3s^{-1}, while the simulated mean flow was 0.034 m^3s^{-1}, ranging from 0.0197 to 0.582 m^3s^{-1}. At gauge B, the observed daily mean flow was 0.049 m^3s^{-1}, with a range of 0.0 to 2.673 m^3s^{-1}, and the simulated mean was 0.038 m^3s^{-1}, with a range of 0.0046 to 2.808 m^3s^{-1} (Figure Aannex4a; Figure Annex 4b).

The average slope length (SLSUBBSN), peak rate adjustment factor in

Table 2
Spectral indices.

Index	Full name	Formulation	S-2 bands	Reference
AWEI	Automated Water Extraction Index	$Blue + 2.5 \bullet Green - 1.5(NIR + SWIR1) - 0.25 \bullet SWIR2$	B2, B3, B8, B11, B12	Feyisa et al., 2014
NDWI	Normalized Difference Water Index	$\frac{Green - NIR}{Green + NIR}$	B3, B8	Mcfeeters, 1996
NDTI	Normalized Difference Turbidity Index	$\frac{Red - Green}{Red + Green}$	B3, B4	Lacaux et al., 2007

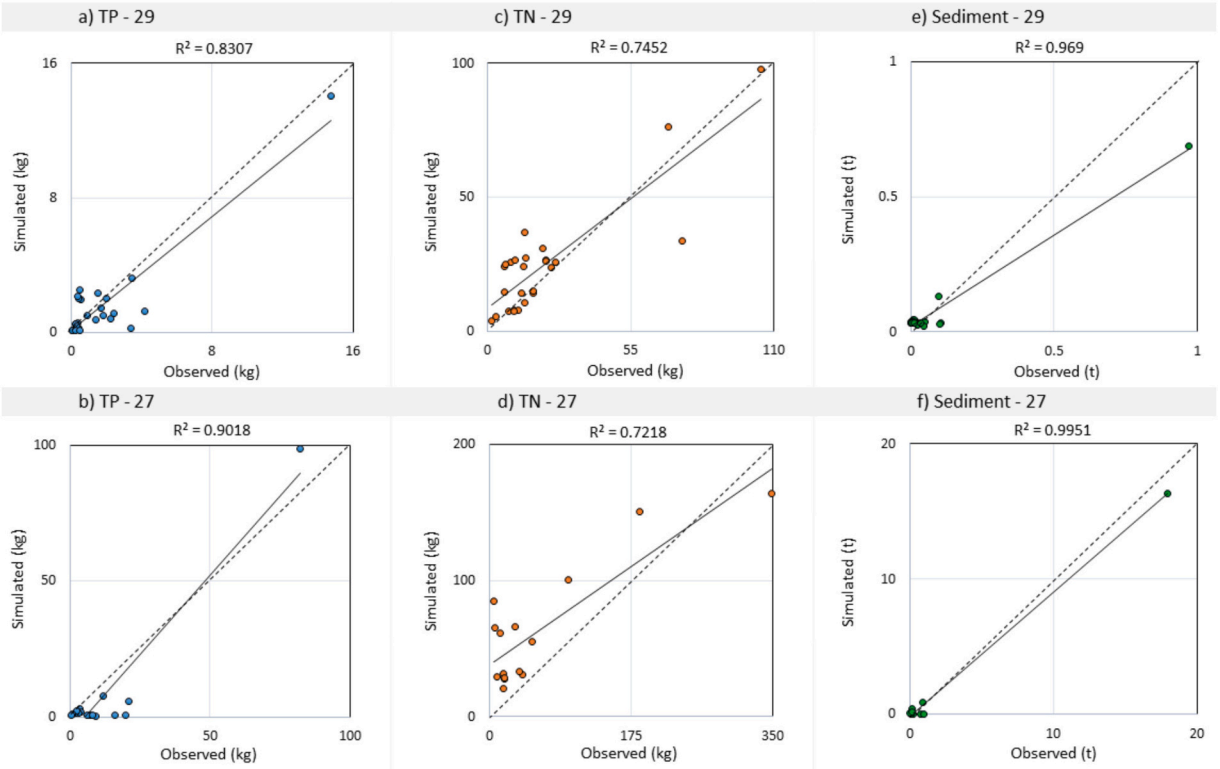

Fig. 2. Daily simulated and observed TP, TN, and sediment at reach 27 (3b,3d,3f) and 29 (3a,3c,3e).

Table 3
Calibrated parameters for the best fit simulation of the Canale d'Aiedda basin at the gauge A (reach 29) and B (reach 27).

Hydrology			Nutrient			Sediment		
Parameter	Fitted value A	Fitted value B	Parameter	Fitted value A	Fitted value B	Parameter	Fitted value A	Fitted value B
v_EVRCH.bsn	0.865*		v_AI1.wwq	0.08*		v_ADJ_PKR.bsn	0.622*	
v_SURLAG.bsn	10.946*		v_AI2.wwq	0.015*		v_RSDCO.bsn	0.074*	
v_TRNSRCH.bsn	0.511*		v_CDN.bsn	0.25*		v_SPCON.bsn	0.003*	
r_CN2.mgt	−0.260	0.210	v_RCN_SUB_BSN.bsn	1.8*		v_SPEXP.bsn	1.499*	
v_BIOMIX.mgt	0.697	0.622	v_NFIXMX.bsn	15*		v_CH_COV1.rte	0.349	0.505
v_ALPHA_BF.gw	0.004	0.294	v_N_UPDIS.bsn	90*		v_CH_COV2.rte	0.456	0.266
v_GW_DELAY.gw	333.824	42.052	v_PHOSKD.bsn	100*		v_CH_ERODMO.rte	0.805	0.224
v_GWQMN.gw	386.109	2222.123	v_PPERCO.bsn	10*		v_LAT_SED.hru	10.985	3424.48
v_REVAPMN.gw	410.453	749.154	v_NPERCO.bsn	2*		r_SLSUBBSN.hru	−0.080	−0.220
v_RCHRG_DP.gw	0.103	0.853	v_PSP.bsn	0.02*		v_USLE_P.mgt	0.087	0.050
v_GW_REVAP.gw	0.171	0.181	v_SDNCO.bsn	1.1*				
r_SOL_K().sol	0.080	−0.098	v_BC1_BSN.bsn	0.55*				
r_SOL_AWC().sol	0.217	−0.101	v_BC2_BSN.bsn	1.1*				
v_SOL_ALB().sol	0.170	0.217	v_BC3_BSN.bsn	0.21*				
r_SOL_Z().sol	0.097	−0.234	v_BC4_BSN.bsn	0.355*				
v_EPCO.hru	0.512	0.894	v_P_UPDIS.bsn	0.5*				
v_ESCO.hru	0.256	0.692	v_FIXCO.bsn	1*				
v_CANMX.hru	1.410	3.138	v_CH_ONCO_BSN.bsn	50*				
v_CANMX.hru	1.260	3.368	v_CH_OPCO_BSN.bsn	50*				
v_CANMX.hru	0.772	0.322	v_RCN.bsn	1*				
v_CANMX.hru	0.372	2.224	v_CMN.bsn	0.001				
v_CANMX.hru		0.067	v_SOL_NO3().chm	75	55			
v_CANMX.hru		2.330	v_SOL_ORGN().chm	5	5			
v_CANMX.hru		3.287	v_SOL_ORGP().chm	5	5			
v_CANMX.hru		4.307	v_SHALLST_N.gw	75	75			
v_CH_K1.sub	107.085	29.669	v_ERORGN.hru	2.5	2.5			
v_CH_N1.sub	17.895	10.069	v_ERORGP.hru	2.5	3			
v_CH_N2.rte	6.817	0.276	v_FRT_SURFACE.mgt	0.6	0.6			
v_CH_K2.rte	0.260	43.230						

* The specific parameter can be adjusted only at the basin level.

the subbasin (ADJ_PKR), and the sediment routing parameter (SPCON and SPEXP) were the most sensitive parameters for sediment predictions. The calibration of TP and TN included several parameters. The most sensitive parameters for nitrogen included the nitrogen uptake distribution parameter (N_UPDIS), the nitrate percolation coefficient (NPERCO), the initial NO_3 concentration in the soil layer (SOL_NO3),

Table 4
Statistical performances of the SWAT model calibration at a daily time step.

Variable	B (Reach 27)			A (Reach 29)		
	R^2	NSE	PBIAS	R^2	NS	PBIAS
FLOW_OUT	0.60	0.58	+23.00	0.50	0.50	0.00
SED_OUT	1.00	0.98	+15.80	0.97	0.88	−0.60
TN	0.72	0.59	−5.0	0.75	0.73	−14.90
TP	0.90	0.77	+35.50	0.83	0.83	+8.00

and the initial organic N concentration in the soil layer (SOL_ORGN). For phosphorus, the key parameters were the phosphorus uptake distribution parameter (P_UPDIS), the phosphorus soil partitioning coefficient (PHOSKD), the phosphorus percolation coefficient (PPERCO), and the initial organic P concentration in the soil layer (SOL_ORGP) (Table 3).

Statistical performances for sediment calibration indicate a strong agreement between observed and simulated values for both gauges (Table 4, Fig. 2). At the basin scale, the annual average sediment load was 0.027 t ha^{-1}. For TP, the results indicated excellent agreement at Gauge A and good performance at Gauge B (Fig. 2). For TN calibration, statistical evaluation showed good performance at gauge A and slightly lower agreement at gauge B (Table 4).

3.2. Spatial and temporal distribution of pollutants

For the year 2023, the annual average sediment load was 0.014 t ha^{-1}. At the subbasin scale simulated value ranged from 0.001 t ha^{-1} to 0.213 t ha^{-1}. These results are far below the limit of soil generation (1.4 t ha^{-1}, Verheijen et al., 2009) indicating that for the study area the soil erosion is not a main issue. For this reason, only the TN and TP loads were further analyzed.

The spatial distribution of TN and TP loads varies across sub-basins, reflecting differences in land cover and management practices. The higher TN loads (~7 to 10 kg $ha^{-1}y^{-1}$) were simulated in the northwestern subbasins, where agricultural land uses are predominant (vineyards, olive groves, and winter wheat) (Table 5, Fig. 3a). Agricultural practices such as fertilizer application and tillage operations are responsible for nutrient and soil particle delivery to the stream. The highest value of TP load was simulated near the basin outlet (0.7 kg $ha^{-1}y^{-1}$), in the subbasin where the vineyard is the prevalent crop production (Table 5, Fig. 3b).

The temporal distribution of TN and TP loads delivered to the sea shows distinct seasonal patterns. The TN load exhibited high values in April and October, while the TP load showed high values in April, October, June, and August. For the remaining months, the nutrient load pattern was stable (Fig. 3c and Fig. 3d). In April and October, the high values of nutrient loads could be related to precipitation and runoff patterns, which enhance the export and transport of nutrients from agricultural lands to the water bodies. The high values of the TP load in June and August are mainly due to WWTPs' discharges because natural runoff is low or absent (Fig. 3c and Fig. 3d).

Table 5
Total Nitrogen (TN) and Total phosphorous (TP) loads for each subbasins for 2023.

Subbasin number	TN (kg ha^{-1})	TP (kg ha^{-1})	Subbasin number	TN (kg ha^{-1})	TP (kg ha^{-1})
1	9.46	0.21	21	1.84	0.13
2	4.11	0.23	22	0.05	0.00
3	7.18	0.39	23	0.05	0.01
4	5.05	0.33	24	0.41	0.04
5	0.91	0.04	25	0.72	0.03
6	0.41	0.01	26	1.94	0.08
7	6.03	0.34	27	2.16	0.10
8	8.40	0.22	28	0.69	0.09
9	0.30	0.01	29	0.05	0.00
10	1.38	0.05	30	2.42	0.70
11	0.75	0.03	31	0.08	0.00
12	2.53	0.14	32	0.05	0.00
13	0.10	0.01	33	0.13	0.00
14	0.24	0.01	34	0.13	0.00
15	0.53	0.04	35	0.01	0.00
16	0.61	0.03	36	1.26	0.27
17	0.90	0.04	37	0.33	0.02
18	1.83	0.18	38	0.08	0.00
19	0.93	0.04	39	0.05	0.00
20	0.99	0.04	40	0.99	0.30

3.3. Plume of pollutants from catchment to sea

The analysis of the flood that occurred on June 10th, 2023, carried out by coupling satellite imagery and SWAT model predictions, provided insights into the transport of sediments and nutrients into the sea during the event. At the basin scale, the rainfall was 29.72 mm, and at the outlet, the streamflow was 0.066 m^3s^{-1}. Sediment load delivered to marine environments was 31.43 t, TN was 19.4 kg, and TP load was 1.43 kg. These results highlight the significant impact of such hydrological events on nutrient and sediment fluxes delivered to the sea.

The water turbidity caused by the flood was mapped for Mar Piccolo and the estuarine area of the d'Aiedda River (Palude la vela). Fig. 4a presents the mean annual NDTI scores for 2022 within the AOI, as well as the NDTI values seven days before (Fig. 4b) and eight days after the rainfall event (Fig. 4c). A stretch image processing based on the pixel values standard deviation (σ) was applied to reduce the gradient range and emphasize the results (Fig. 4d, e, f).

The NDTI values calculated for the AOI, along with their range, are summarized in Table 5a. A significant increase in NDTI was observed across the Mar Piccolo water body before and after the selected flood event, compared to the mean annual value recorded in 2022 (Fig. 4, Table 6). Outliers were identified in the maximum values (Table 6a), as both June measurements were lower than the annual averages. Additionally, the highest NDTI recorded after the flood event was lower than that observed before the event. This discrepancy can be attributed to isolated pixels representing small surface areas rather than the entire study region. For this reason, the detected average values are more significant than the minimum and maximum values. The mean values of NDTI progressively increases from yearly averages to June observation, both for Mar Piccolo and D'Aiedda estuarine zone, where the NDTI increased by more than 0.05 units (Table 6b).

The NDTI difference (before and after the flood) was significantly high in the southeastern area, in the surrounding waters near the d'Aiedda outlet (Fig. 5a), where the current tends to veer left. NDTI values are relatively low in the center of Mar Piccolo and higher along the coast. Fig. 5b illustrates the water surface, where the NDTI increased by more than 0.05 units. This threshold was chosen to distinguish between general water turbidity and turbidity caused by rain events.

The NDTI values for areas with an increase of more than 0.05 units, predominantly near the estuarine channel, are summarized in Table 5b. A rising trend is observed in the extreme and average values after the flood event.

4. Discussion

4.1. Modeling hydrology, sediment, and nutrient transport

The SWAT model was successfully capable of simulating hydrological processes, sediment transport, and nutrient dynamics in the Canale d'Aiedda basin with satisfactory to good statistical performance criteria. The model's performance in correctly describing the hydrological dynamics of this intermittent Mediterranean stream is important, as it is common that intermittent streams can be difficult to model because their flow regimes can be variable (De Girolamo et al., 2017; Ricci et al., 2023). These results confirm observations in other similar studies in the Mediterranean region where SWAT was successfully employed to model

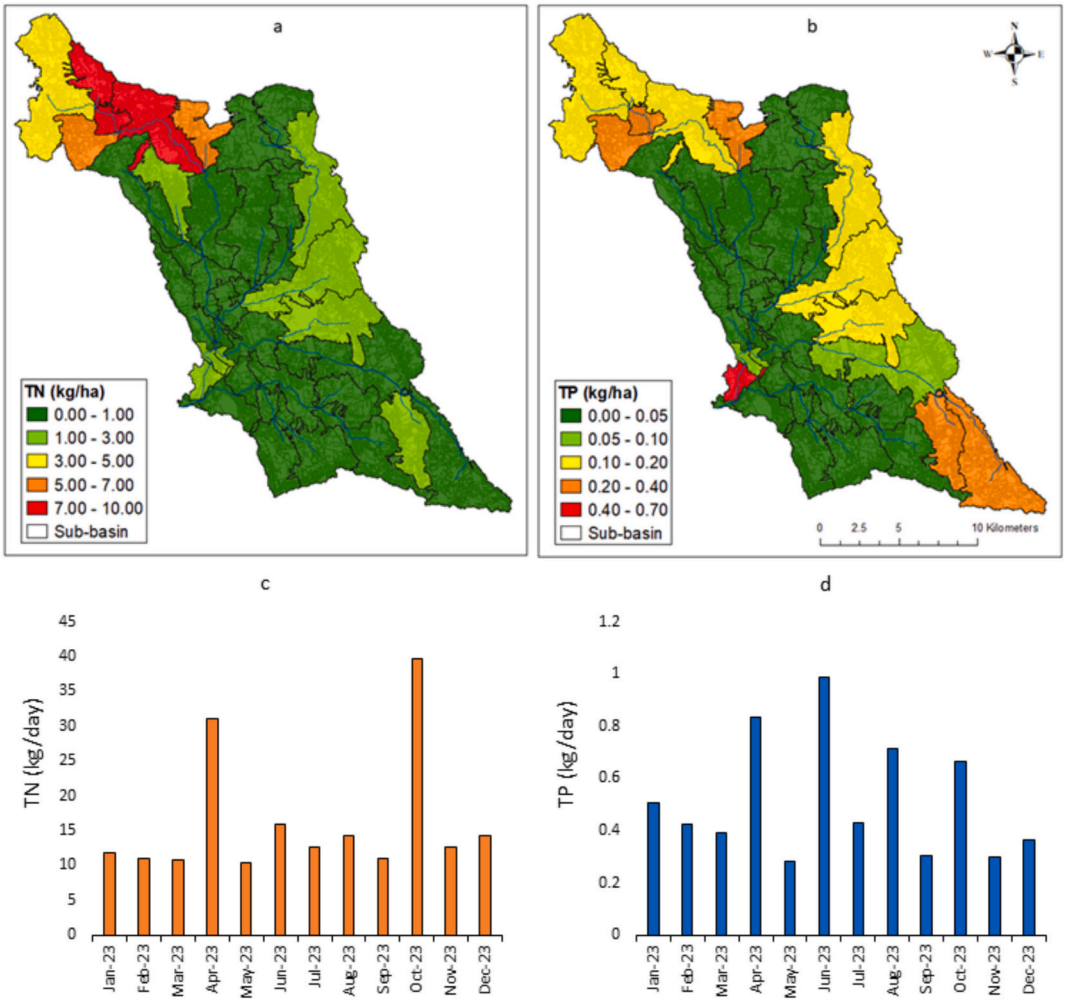

Fig. 3. Spatial distribution of the annual load of TN a) and TP b), and temporal distribution of the average monthly load represented in c) and d) estimated for 2023.

streamflow in systems under high temporal variability (Centanni et al., 2024; Molina-Navarro et al., 2014; Papatheodoulou et al., 2013).

The spatial pattern of nutrient loads among sub-basins indicated clear patterns following land use, as would be expected because of the prevalence of agricultural land use in the basin. The highest TN loads (~10 kg $ha^{-1}y^{-1}$) were simulated in northwest sub-basins with dominance of vineyard, olive grove, and winter wheat, while the highest TP loads (0.7 kg $ha^{-1}y^{-1}$) were projected at the outlet of the basin in areas dominated by vineyards. These are consistent with current studies that have established agriculture as a key cause of nutrient loads in Mediterranean watersheds (D'Ambrosio et al., 2019; Malagó et al., 2019; Pisinaras et al., 2019; Pulighe et al., 2020).

The loads of TN and TP simulated in this study are comparable to the rate of loading that is identified in other similar Mediterranean agricultural basins. For instance, De Girolamo et al. (2019) noted a general mean TP yield of 0.86 kg ha^{-1} yr^{-1} for the southern Sardinian Rio Mannu basin, while Pulighe et al. (2020) estimated for TN and TP, total amounts of 4.8 and 1.18 kg ha^{-1} y^{-1}, respectively.

Our findings support Carvalho-Santos et al. (2016), who report in a corresponding Mediterranean watershed in Portugal with TN and TP loads of approximately 1.04 and 1.09 kg ha^{-1} y^{-1}, respectively. da Burigato Costa et al. (2019), in a watershed located in central Italy, found values of TN ranging from 0 to 41 kg ha^{-1} y^{-1}, which are higher in the maximum, and of TP ranging from and to 0 to 0.71 kg ha^{-1} y^{-1}. Moreover, Malagó et al. (2019) estimated similar average values for TN (3.74 kg ha^{-1} y^{-1}) and TP (0.22 kg ha^{-1} y^{-1}) the whole Mediterranean sea drainage area.

Contrastingly, Panagopoulos et al. (2011) reported considerably higher mean annual TN export (20 kg ha^{-1} y^{-1}) in a Greek catchment. Similarly, Salim Aoubid and Opp (2023) found loads of TN ranging from 0.27 to 65 kg ha^{-1} y^{-1} and of TP from 0.01 to 16 kg ha^{-1} y^{-1}. Such a large disparity is likely the result of the much larger watershed area and its distinct characteristics. Comparability with these studies suggests that our results reflect average nutrient export regimes from representative Mediterranean agricultural land covers dominated by permanent crops such as vineyards and olive groves.

Seasonal cycles of nutrient loading in this work are a product of the dynamic coupling between agricultural activities and hydrologic processes. Maximum TN and TP loads in April and October occur when there are high precipitation rates along with agricultural activities (fertilizer application and tillage), which enhance the mobilization and transport of nutrients. This is supported by the observation of Fouilland et al. (2012), whose research highlighted the importance of rainy season trends to nutrient export from Mediterranean catchments. The elevated TP loads during summer months (June and August), despite low natural runoff, augment the data to confirm that WWTPs turn into predominant phosphorus loading sources during dry seasons, which validates findings by Magand et al. (2020) regarding the influence of point sources under low flow regimes in intermittent streams.

4.2. Remote sensing approach for plume detection

The application of remote sensing techniques, using the NDTI, is a methodological advance in coastal plume detection for intermittent

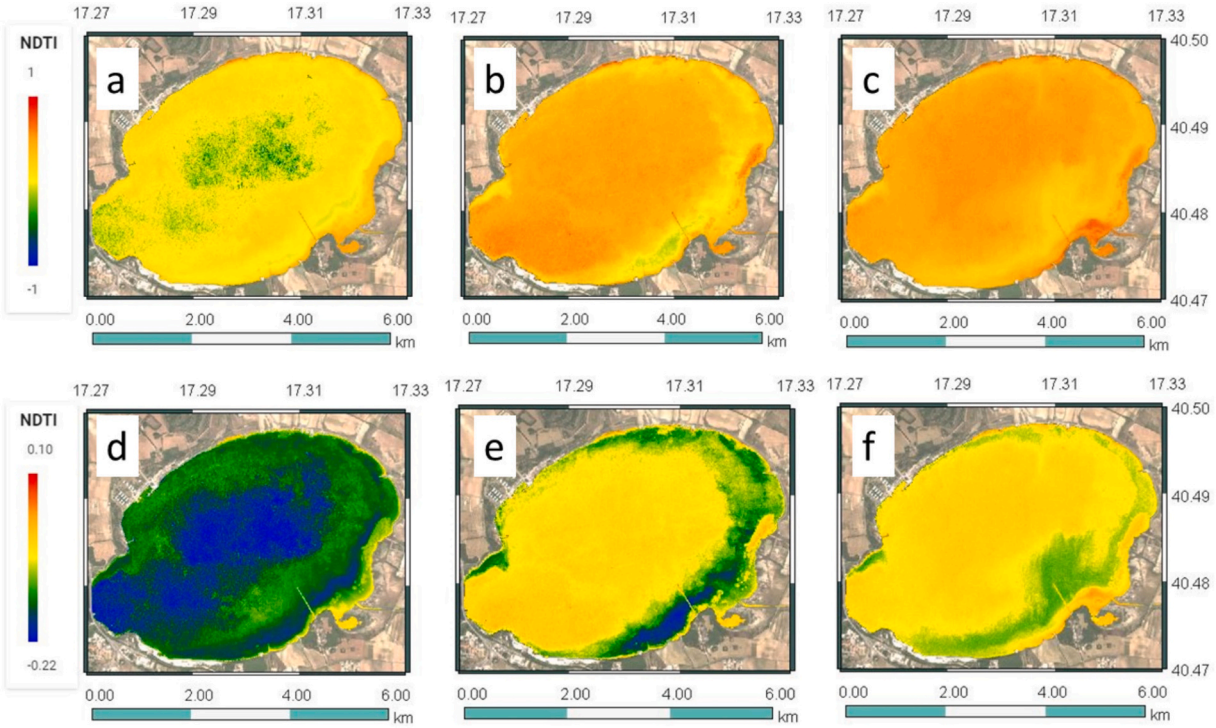

Fig. 4. Annual mean scores of NDTI of Mar Piccolo (a, d); NDTI scores before (b, e) and after (c, f) flood event (June 10th, 2023), respectively. A stretch of 3σ was applied to reduce the gradient range (d, e, f).

Table 6
NDTI values for (a) Mar Piccolo and, (b) D'Aiedda estuarine.

	(a) Mar Piccolo			(b) D'Aiedda channel estuarine		
	min	max	mean	min	max	mean
Year (2022)	−0.4463	0.0947	−0.1603	−0.2167	−0.0028	−0.1506
Jun 3, 2023	−0.2233	0.0843	−0.0664	−0.2233	−0.0063	−0.1488
Jun 18, 2023	−0.1323	0.0634	−0.0522	−0.128	0.0634	−0.0636
Difference (18–3 Jun)	−0.1388	0.1666	0.0143	0.06	0.1666	0.0852

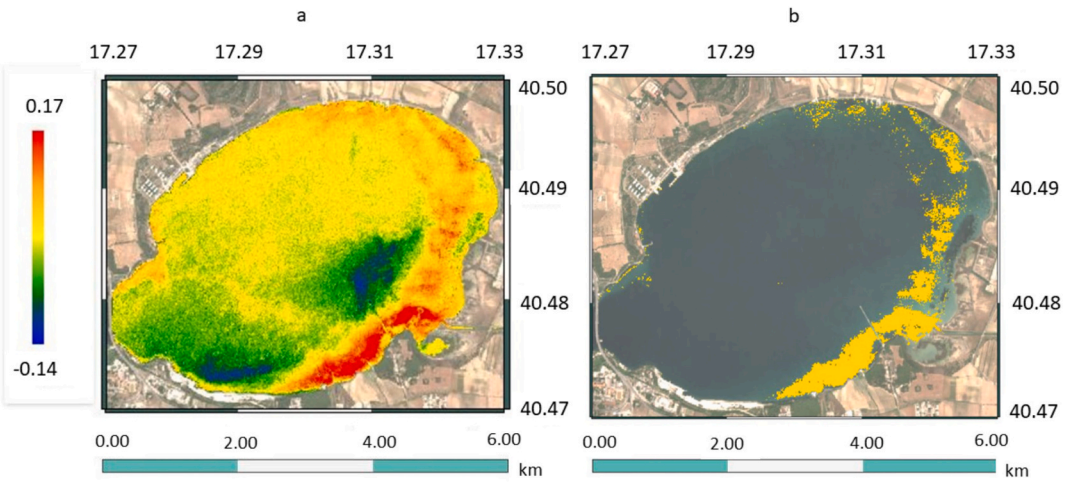

Fig. 5. NDTI differences between before and after the flood event (June 10th, 2023) (a) and NDTI increasing more than 0.05 units (b).

streams. Selection of Sentinel-2 imagery is an appropriate compromise between spatial resolution (10-20 m) and frequency (revisit every 5 days) to enable relative small-scale detection of those plumes likely missed by coarser-resolution satellites such as MODIS or Landsat. This approach is also consistent with the results reported by Dogliotti et al. (2015), who emphasized high spatial resolution requirements in monitoring turbidity in coastal and inland small water bodies. Sentinel-2 is obfuscated by clouds, which poses a significant challenge when tracking

water turbidity during rainfall events under persistent cloud conditions. This aspect limited the availability of images in this study. To address this limitation, Nguyen et al. (2020) proposed a solution by harmonizing data from multiple satellite sources, including Landsat 7 and Sentinel-2. Furthermore, Caballero et al. (2022) suggested that the use of ACOLITE (Vanhellemont and Ruddick, 2014; Vanhellmont and Ruddick, 2016), a generic processor developed for coastal and inland water applications, is effective in successfully removing clouds and sun glints without eliminating cloud shadows.

Comparative water index testing (AWEI and NDWI) of determining water surface areas revealed NDWI to be slightly more accurate over the southeastern corner of the study area, again substantiating the premise that the choice of index is relative to a specific coastal environment. This conclusion is upheld by Mcfeeters (1996) original argument that NDWI possesses inherent benefits when working within turbid coastal water bodies, where suspended sediment penetrates more so by the green band utilized by NDWI than by the blue band utilized in AWEI.

In this work, the spectral assessment of NDTI, following a selected flood event, revealed significant spatial variations of turbidity within Mar Piccolo. The trend of sequence towards higher values of NDTI from annual means to post-flood (Table 5) provides quantitative evidence for plume formation. The sharp increase in NDTI values (+0.0143 units for Mar Piccolo and + 0.0852 units for the D'Aiedda channel estuarine) bears witness to the sensitivity of this spectral index to water turbidity variations, in line with work by Lacaux et al. (2007) and with the same magnitude of change in NDTI measured after precipitation.

The spatial distribution of the plume, with higher turbidity concentrated in the southeastern area near the d'Aiedda outlet (Fig. 5a), agrees with hydrodynamic principles of plume formation. The asymmetric distribution, with higher turbidity observed on the left side of the channel outlet, was not expected and reflects the influence of tidal currents on plume dynamics (De Pascalis et al., 2016). Similar asymmetric patterns have been observed by Baldoni et al. (2022) and Salcedo-Castro et al. (2023), who attributed such distributions to the Coriolis effect and local circulation patterns. The finding suggests the complex three-dimensional nature of coastal plume dynamics and the utility of satellite-based observation for its detection as spatial heterogeneities.

The trend of growing turbidity closer to the coast compared to the interior of Mar Piccolo has been observed following coastal plume dynamics documented by Spicer et al. (2021), who described weak vertical mixing in areas of reduced tidal activity. Our designation of areas of NDTI grows above 0.05 units (Fig. 5b) provides an approach to distinguishing event-induced turbidity from background variability, offering a quantitative technique for plume size mapping that would be applicable routinely in the future.

The integration of SWAT-modeled sediment outputs with NDTI measurements demonstrates the complementary nature of these approaches. While the SWAT model provided quantitative estimates of sediment loads (31.43 t), the NDTI analysis revealed the spatial fate of these sediments once they entered the coastal system. This integration addresses a significant knowledge gap in the understanding of the source-to-sea continuum of sediment transport, particularly in intermittent Mediterranean streams where conventional monitoring techniques are often limited by the episodic nature of flow events.

4.3. Integrated watershed-coastal management implications

The combined use of ecohydrological modeling and remote sensing in this study offers a novel approach for understanding the fate of pollutants from catchment to coast. It addresses a significant gap in the literature regarding intermittent streams and their impact on coastal ecosystems. Previous studies have often focused separately on either watershed processes or coastal plume dynamics, with limited integration between these domains (Baldoni et al., 2022; Salcedo-Castro et al., 2023). Our integrated approach provides a more comprehensive understanding of the entire source-to-sea continuum, which is essential for effective water quality management.

The identification of critical source areas for nutrients within the basin provides valuable information for targeted management interventions. The high nutrient export from agricultural sub-basins, particularly those dominated by vineyards and olive groves (Babaei et al., 2019; Khanal et al., 2018), suggests that implementing improved agricultural practices in these areas could significantly reduce nutrient loading to the Mar Piccolo. Similar conclusions have been drawn by Strauss et al. (2007) and Mtibaa et al. (2018), who emphasized the importance of targeting critical source areas for cost-effective watershed management.

The observed impacts of point sources during dry periods highlight the need for improved wastewater treatment. This finding is consistent with recommendations by Magand et al. (2020) and Ricci et al. (2022) regarding the management of point sources in intermittent streams. The seasonal patterns of nutrient loading suggest that management strategies should be tailored to address different sources depending on the time of year, with a focus on diffuse agricultural sources during wet periods and point sources during dry periods.

The analysis of the flash flood showed that these events may be critical for water quality (Fouilland et al., 2012), demonstrating the episodic nature of sediment transport in Mediterranean intermittent river systems, as observed by Buendia et al. (2016). In the dry season (summer and autumn), flash floods are very common in the Mediterranean Region (Llasat et al., 2014; Tramblay et al., 2023), leading to the washing out of a large amount of sediment and nutrients into the stream and, consequently, to the sea. The plume formed by these events can impact the quality of the coastal water bodies (Rosa et al., 2022; Sauvage et al., 2018). Moreover, in areas with reduced tidal influence and low wind stress, such as the Mar Piccolo, stratification within plumes can limit the mixing of sediment and affect sediment transport processes in the coastal environment (Spicer et al., 2021). The importance of flash floods in sediment and nutrient transport emphasizes the need for management approaches that address these episodic events. Traditional management approaches (i.e. plowing up and down slopes, no reduced tillage or crop residue management or cover cropping) often focus on average conditions and may not adequately address the significant pollution loads delivered during extreme events. This finding supports the conclusions of Tramblay et al. (2021a, 2021b) regarding the importance of considering hydrological extremes in Mediterranean watershed management.

The observed plume dynamics in the Mar Piccolo highlight the vulnerability of this semi-enclosed marine basin to terrestrial inputs, which is particularly concerning given its ecological importance and the presence of mussel farming activities. The spatial distribution of turbidity suggests that sediments and associated pollutants may impact specific areas of the basin more severely than others, which should be considered in coastal management and conservation efforts. Similar concerns have been raised by Petrosillo et al. (2023) regarding the balance between economic activities and environmental protection in Mar Piccolo.

4.4. Methodological strengths and limitations

Combining SWAT modeling with remote sensing represents a notable advancement in studying source-to-sea systems, despite several limitations. Discrete sediment sampling for both sediment and nutrients may miss the high variability of intermittent streams, with more intensive storm event monitoring needed in future work (De Girolamo et al., 2019). While our model showed satisfactory performance metrics, continuous monitoring would improve reliability for extreme events. The remote sensing approach using NDTI requires ground-truthing to establish quantitative relationships between index values and actual suspended sediment concentrations, as satellite-based indices struggle with extreme values (Dewantoro et al., 2024; Tavora et al., 2023).

Sentinel-2's 5-day revisit time often misses rapidly evolving plume dynamics, particularly problematic for flash floods in Mediterranean systems where conditions change within hours. Despite these constraints, this integrated approach bridges the watershed-coastal monitoring divide—SWAT providing continuous temporal predictions at limited spatial points while satellite imaging offers extensive spatial coverage at discrete intervals. This combination proves particularly valuable for watersheds with intermittent streams where conventional monitoring struggles with variable flow regimes (Arnold, 2012).

5. Conclusion

This study demonstrates the efficacy of integrating ecohydrological modeling with remote sensing for tracking pollutant dynamics from catchment to coast. The SWAT model successfully identified critical source areas of nutrients within the Canale d'Aiedda basin, with agricultural lands—particularly vineyards and olive groves—contributing the highest TN loads (10 kg $ha^{-1}y^{-1}$) and TP loads (0.7 kg $ha^{-1}y^{-1}$). Temporal patterns revealed distinct seasonal variability, with peak nutrient transport occurring during spring and autumn rainfall events. The June 2023 flash flood analysis highlighted the episodic nature of pollutant transport in Mediterranean intermittent streams, delivering substantial loads (19.4 kg TN, 1.43 kg TP, and 31.43 t sediments) to the Mar Piccolo. Remote sensing analysis using NDTI effectively captured the spatial distribution of the resulting sediment plume, revealing asymmetric dispersion influenced by local circulation patterns.

While our approach addresses significant knowledge gaps regarding the source-to-sea continuum, several limitations remain. The discrete water quality sampling likely missed peak concentrations during extreme events, and Sentinel-2's temporal resolution cannot fully capture rapidly evolving plume dynamics. Future research should incorporate high-frequency water quality monitoring during storm events and explore integration with hydrodynamic models to better predict plume behavior in coastal waters. Nevertheless, this integrated methodology offers valuable insights for watershed management, suggesting targeted interventions for agricultural practices in critical source areas and improved wastewater treatment to mitigate impacts on coastal ecosystems, particularly in vulnerable semi-enclosed basins like the Mar Piccolo.

Declaration of generative AI in scientific writing

The Authors declare that no generative AI was used for the scientific writing.

CRediT authorship contribution statement

Marco Centanni: Writing – original draft, Visualization, Software, Methodology, Investigation, Formal analysis. **Rose Mary:** Writing – original draft, Visualization, Data curation. **Giovanni Romano:** Writing – original draft, Visualization, Software, Investigation, Formal analysis. **Giovanni Francesco Ricci:** Writing – review & editing, Writing – original draft, Methodology, Investigation, Formal analysis, Data curation, Conceptualization. **Ossama M.M. Abdelwahab:** Writing – review & editing, Writing – original draft, Data curation. **Julio Pérez-Sánchez:** Writing – review & editing, Writing – original draft, Methodology. **Anna Maria De Girolamo:** Writing – review & editing, Writing – original draft, Validation, Supervision, Methodology, Conceptualization. **Francesco Gentile:** Writing – original draft, Supervision, Resources, Project administration, Funding acquisition.

Funding

The author(s) declare that financial support was received for the research and/or publication of this article. This study was carried out within the Agritech National Research Center and received funding from the European Union Next-Generation EU (PIANO NAZIONALE DI RIPRESA E RESILIENZA (PNRR)—MISSIONE 4 COMPONENTE 2, INVESTIMENTO 1.4—D.D. 1032 17/06/2022, CN00000022). This manuscript reflects only the authors' views and opinions, neither the European Union nor the European Commission can be considered responsible for them.

Data availability

The raw data supporting the conclusions of this article are available through this link: https://zenodo.org/records/16418182. DOI https://doi.org/10.5281/zenodo.16418181

References

Abbaspour, K.C., Rouholahnejad, E., Vaghefi, S., Srinivasan, R., Yang, H., Kløve, B., 2015. A continental-scale hydrology and water quality model for Europe: calibration and uncertainty of a high-resolution large-scale SWAT model. J. Hydrol. 524, 733–752. https://doi.org/10.1016/j.jhydrol.2015.03.027.

Álvarez-Romero, J., Devlin, M., Silva, E., Petus, C., Ban, N., Pressey, R., Kool, J., Roberts, J., Cerdeira-Estrada, S., Wenger, A., Brodie, J., 2013. A novel approach to model exposure of coastal-marine ecosystems to riverine flood plumes based on remote sensing techniques. J. Environ. Manage. 119C, 194–207. https://doi.org/10.1016/j.jenvman.2013.01.036.

Arnold, J.G., 2012. SWAT: Model Use, Calibration, and Validation. American Society of Agricultural and Biological Engineers, St. Joseph, Michigan 55 (4), 1491–1508. https://doi.org/10.13031/2013.42256.

Arnold, J.G., Srinivasan, R., Muttiah, R.S., Williams, J.R., 1998. Large area hydrologic modeling and assessment part I: model development. JAWRA Journal of the American Water Resources Association 34 (1), 73–89. https://doi.org/10.1111/j.1752-1688.1998.tb05961.x.

Babaei, H., Nazari-Sharabian, M., Karakouzian, M., Ahmad, S., 2019. Identification of critical source areas (CSAs) and evaluation of best management practices (BMPs) in controlling eutrophication in the Dez River basin. Environments 6 (2). https://doi.org/10.3390/environments6020020. Article 2.

Bagnold, R.A., 1977. Bed load transport by natural rivers. Water Resour. Res. 13 (2), 303–312. https://doi.org/10.1029/WR013i002p00303.

Baldoni, A., Perugini, E., Penna, P., Parlagreco, L., Brocchini, M., 2022. A comprehensive study of the river plume in a microtidal setting. Estuar. Coast. Shelf Sci. 275, 107995. https://doi.org/10.1016/j.ecss.2022.107995.

Borg Galea, A., Sadler, J.P., Hannah, D.M., Datry, T., Dugdale, S.J., 2019. Mediterranean intermittent rivers and ephemeral streams: challenges in monitoring complexity. Ecohydrology 12 (8), e2149. https://doi.org/10.1002/eco.2149.

Brown, L., Barnwell, T., 1987. The enhanced stream water quality models QUAL2E /and QUAL2E-UNCAS: documentation and user manual. Environmental Protection Agency. EPA/600/3-87/007.

Buendia, C., Bussi, G., Tuset, J., Vericat, D., Sabater, S., Palau, A., Batalla, R.J., 2016. Effects of afforestation on runoff and sediment load in an upland Mediterranean catchment. Sci. Total Environ. 540, 144–157. https://doi.org/10.1016/j.scitotenv.2015.07.005.

Caballero, I., Román, A., Tovar-Sánchez, A., Navarro, G., 2022. Water quality monitoring with Sentinel-2 and Landsat-8 satellites during the 2021 volcanic eruption in La Palma (Canary Islands). Sci. Total Environ. 822, 153433. https://doi.org/10.1016/j.scitotenv.2022.153433.

Cabezas-Rabadán, C., Rodilla, M., Pardo-Pascual, J.E., Herrera-Racionero, P., 2019. Assessing users' expectations and perceptions on different beach types and the need for diverse management frameworks along the Western Mediterranean. Land Use Policy 81, 219–231. https://doi.org/10.1016/j.landusepol.2018.10.027.

Carvalho-Santos, C., Nunes, J.P., Monteiro, A.T., Hein, L., Honrado, J.P., 2016. Assessing the effects of land cover and future climate conditions on the provision of hydrological services in a medium-sized watershed of Portugal. Hydrol. Process. 30 (5), 720–738. https://doi.org/10.1002/hyp.10621.

Centanni, M., Ricci, G.F., De Girolamo, A.M., Gentile, F., 2024. Modeling pesticides and ecotoxicological risk assessment in an intermittent river using SWAT. Sci. Rep. 14 (1), 6389. https://doi.org/10.1038/s41598-024-56991-6.

da Burigato Costa, C.M.S., da Silva Marques, L., Almeida, A.K., Leite, I.R., de Almeida, I. K., 2019. Applicability of water quality models around the world-a review. Environ. Sci. Pollut. Res. Int. 26 (36), 36141–36162. https://doi.org/10.1007/s11356-019-06637-2.

Dagg, M., Benner, R., Lohrenz, S., Lawrence, D., 2004. Transformation of dissolved and particulate materials on continental shelves influenced by large rivers: plume processes. Cont. Shelf Res. 24 (7), 833–858. https://doi.org/10.1016/j.csr.2004.02.003.

D'Ambrosio, E., De Girolamo, A.M., Spanò, M., Corbelli, V., Capasso, G., Morea, M., Velardo, R., Abdelwahab, O.M.M., Lonigro, A., Milillo, F., Ricci, G.F., Romano, G., Calabrese, A., Casale, B., Mauro, R., Pappagallo, G., Gentile, F., 2019. A spatial analysis to define data requirements for hydrological and water quality models in data-limited regions. Water 11(2), Article 2. https://doi.org/10.3390/w11020267.

D'Ambrosio, E., Gentile, F., De Girolamo, A.M., 2020. Assessing the sustainability in water use at the basin scale through water footprint indicators. J. Clean. Prod. 244, 118847. https://doi.org/10.1016/j.jclepro.2019.118847.

De Girolamo, A.M., Barca, E., Pappagallo, G., Lo Porto, A., 2017. Simulating ecologically relevant hydrological indicators in a temporary river system. Agric Water Manag 180, 194–204. https://doi.org/10.1016/j.agwat.2016.05.034.

De Girolamo, A.M., Spanò, M., Ersilia, D., Ricci, G.F., Gentile, F., 2019. Developing a nitrogen load apportionment tool: theory and application. Agric Water Manag 226 (C). https://econpapers.repec.org/article/eeeagiwat/v_3a226_3ay_3a2019_3ai_3ac_3as0378377419310571.htm.

De Pascalis, F., Petrizzo, A., Ghezzo, M., et al., 2016. Estuarine circulation in the Taranto seas. Environ. Sci. Pollut. Res. 23, 12515–12534. https://doi.org/10.1007/s11356-015-5389-3.

Delgado-Fernandez, I., O'Keeffe, N., Davidson-Arnott, R.G.D., 2019. Natural and human controls on dune vegetation cover and disturbance. Sci. Total Environ. 672, 643–656. https://doi.org/10.1016/j.scitotenv.2019.03.494.

Devlin, M.J., Petus, C., Da Silva, E., Tracey, D., Wolff, N.H., Waterhouse, J., Brodie, J., 2015. Water quality and river plume monitoring in the great barrier reef: an overview of methods based on ocean colour satellite data. Remote Sens 7 (10). https://doi.org/10.3390/rs71012909. Article 10.

Dewantoro, M.D.R., Ulfa, M., Supatmanto, B.D., 2024. Water turbidity mapping using Sentinel-2A imagery and cloud based Google Earth Engine in Saguling reservoir. IOP Conference Series: Earth and Environmental Science 1343 (1), 012027. https://doi.org/10.1088/1755-1315/1343/1/012027.

Dogliotti, A.I., Ruddick, K.G., Nechad, B., Doxaran, D., Knaeps, E., 2015. A single algorithm to retrieve turbidity from remotely-sensed data in all coastal and estuarine waters. Remote Sens. Environ. 156, 157–168. https://doi.org/10.1016/j.rse.2014.09.020.

European Space Agency(ESA), 2015. Sentinel-2 User Guide.

Feyisa, G.L., Meilby, H., Fensholt, R., Proud, S.R., 2014. Automated water extraction index: A new technique for surface water mapping using Landsat imagery. Remote Sens. Environ. 140, 23–35. https://doi.org/10.1016/j.rse.2013.08.029.

Fortesa, J., Ricci, G.F., García-Comendador, J., Gentile, F., Estrany, J., Sauquet, E., Datry, T., De Girolamo, A.M., 2021. Analysing hydrological and sediment transport regime in two Mediterranean intermittent rivers. CATENA 196, 104865. https://doi.org/10.1016/j.catena.2020.104865.

Fouilland, E., Trottet, A., Bancon-Montigny, C., Bouvy, M., Le Floc'h, E., Gonzalez, J.-L., Hatey, E., Mas, S., Mostajir, B., Nouguier, J., Pecqueur, D., Rochelle-Newall, E., Rodier, C., Roques, C., Salles, C., Tournoud, M.-G., Vidussi, F., 2012. Impact of a river flash flood on microbial carbon and nitrogen production in a Mediterranean lagoon (Thau lagoon, France). Estuar. Coast. Shelf Sci. 113, 192–204. https://doi.org/10.1016/j.ecss.2012.08.004.

Gancheva, I., Peneva, E., Slabakova, V., 2021. Detecting the surface signature of riverine and effluent plumes along the Bulgarian Black Sea coast using satellite data. Remote Sensing 13 (20). https://doi.org/10.3390/rs13204094. Article 20.

González-Ortegón, E., Laiz, I., Sánchez-Quiles, D., Cobelo-Garcia, A., Tovar-Sánchez, A., 2019. Trace metal characterization and fluxes from the Guadiana, Tinto-Odiel and Guadalquivir estuaries to the Gulf of Cadiz. Sci. Total Environ. 650, 2454–2466. https://doi.org/10.1016/j.scitotenv.2018.09.290.

Grizzetti, B., Liquete, C., Pistocchi, A., Vigiak, O., Zulian, G., Bouraoui, F., De Roo, A., Cardoso, A.C., 2019. Relationship between ecological condition and ecosystem services in European rivers, lakes and coastal waters. Sci. Total Environ. 671, 452–465. https://doi.org/10.1016/j.scitotenv.2019.03.155.

Hargreaves, G.H., Samani, Z.A., 1985. Reference crop evapotranspiration from temperature. American Society of Agricultural and Biological Engineers, St. Joseph, Michigan 1 (2), 96–99. https://doi.org/10.13031/2013.26773.

Horner-Devine, A.R., Hetland, R.D., MacDonald, D.G., 2015. Mixing and transport in Coastal River plumes. Annual Review of Fluid Mechanics 47, 569–594. https://doi.org/10.1146/annurev-fluid-010313-141408.

Joumar, N., Nabih, S., Chatzipavlis, A., Velegrakis, A., Hasiotis, T., Tzoraki, O., Stitou El Messari, J.E., Benaabidate, L., 2023. A qualitative assessment of river plumes coupling SWAT model simulations and a beach optical monitoring system. Hydrology 10 (2). https://doi.org/10.3390/hydrology10020038. Article 2.

Kaplan, G., Yalcinkaya, F., Altıok, E., Pietrelli, A., Nastro, R.A., Lovecchio, N., Ieropoulos, I.A., Tsipa, A., 2024. The role of remote sensing in the evolution of water pollution detection and monitoring: A comprehensive review. Physics and Chemistry of the Earth, Parts A/B/C 136, 103712. https://doi.org/10.1016/j.pce.2024.103712.

Kastridis, A., Kirkenidis, C., Sapountzis, M., 2020. An integrated approach of flash flood analysis in ungauged Mediterranean watersheds using post-flood surveys and unmanned aerial vehicles. Hydrol. Process. 34 (25), 4920–4939. https://doi.org/10.1002/hyp.13913.

Khanal, S., Lal, R., Kharel, G., Fulton, J., 2018. Identification and classification of critical soil and water conservation areas in the Muskingum River basin in Ohio. J. Soil Water Conserv. 73, 213–226. https://doi.org/10.2489/jswc.73.2.213.

Lacaux, J.P., Tourre, Y.M., Vignolles, C., Ndione, J.A., Lafaye, M., 2007. Classification of ponds from high-spatial resolution remote sensing: application to Rift Valley fever epidemics in Senegal. Remote Sens. Environ. 106 (1), 66–74. https://doi.org/10.1016/j.rse.2006.07.012.

Le Page, M., Fakir, Y., Aouissi, J., 2020. Chapter 7—Modeling for integrated water resources management in the Mediterranean region. In: Zribi, M., Brocca, L., Tramblay, Y., Molle, F. (Eds.), Water Resources in the Mediterranean Region. Elsevier, pp. 157–190. https://doi.org/10.1016/B978-0-12-818086-0.00007-8.

Lega, M., Endreny, T., 2016. Quantifying the environmental impact of pollutant plumes from coastal rivers with remote sensing and river basin modelling. Int. J. Sustain. Dev. Plan. 11, 651–662. https://doi.org/10.2495/SDP-V11-N5-651-662.

Li, J., Carlson, B.E., Lacis, A.A., 2014. Application of spectral analysis techniques to the intercomparison of aerosol data – part 4: synthesized analysis of multisensor satellite and ground-based AOD measurements using combined maximum covariance analysis. Atmos. Meas. Tech. 7 (8), 2531–2549. https://doi.org/10.5194/amt-7-2531-2014.

Liu, J., Dietz, T., Carpenter, S.R., Alberti, M., Folke, C., Moran, E., Pell, A.N., Deadman, P., Kratz, T., Lubchenco, J., Ostrom, E., Ouyang, Z., Provencher, W., Redman, C.L., Schneider, S.H., Taylor, W.W., 2007. Complexity of coupled human and natural systems. Science 317 (5844), 1513–1516. https://doi.org/10.1126/science.1144004.

Llasat, M.C., Marcos, R., Llasat-Botija, M., Gilabert, J., Turco, M., Quintana-Seguí, P., 2014. Flash flood evolution in North-Western Mediterranean. Atmos. Res. 149, 230–243. https://doi.org/10.1016/j.atmosres.2014.05.024.

Magand, C., Alves, M.H., Calleja, E., Datry, T., Dörflinger, G., England, J., Gallart, F., Gómez, R., Jordà-Capdevila, D., Martí, E., Munné, A., Pastor, V.A., Stubbington, R., Tziortzis, I., Von Schiller, D., 2020. Intermittent rivers and ephemeral streams: What water managers need to know. https://digital.csic.es/handle/10261/214789.

Malagó, A., Bouraoui, F., Grizzetti, B., De Roo, A., 2019. Modelling nutrient fluxes into the Mediterranean Sea. Journal of Hydrology: Regional Studies 22, 100592. https://doi.org/10.1016/j.ejrh.2019.01.004.

Mallin, M.A., Turner, M.I.H., McIver, M.R., Toothman, B.R., Freeman, H.C., 2016. Significant reduction of fecal Bacteria and suspended solids loading by coastal best management practices. J. Coast. Res. 32 (4), 923–931. https://doi.org/10.2112/JCOASTRES-D-15-00195.1.

Mcfeeters, S.K., 1996. The use of the normalized difference water index (NDWI) in the delineation of open water features. International Journal of Remote Sensing 17 (7), 1425–1432. https://doi.org/10.1080/01431169608948714.

Mendes, R., Sousa, M.C., deCastro, M., Gómez-Gesteira, M., Dias, J.M., 2016. New insights into the Western Iberian buoyant plume: interaction between the Douro and Minho River plumes under winter conditions. Prog. Oceanogr. 141, 30–43. https://doi.org/10.1016/j.pocean.2015.11.006.

Molina-Navarro, E., Martínez-Pérez, S., Sastre-Merlín, A., Bienes-Allas, R., 2014. Hydrologic modeling in a small mediterranean basin as a tool to assess the feasibility of a limno-reservoir. J. Environ. Qual. 43 (1), 121–131. https://doi.org/10.2134/jeq2011.0360.

Moriasi, D., Arnold, J., Van Liew, M., Bingner, R., Harmel, R.D., Veith, T., 2007. Model evaluation guidelines for systematic quantification of accuracy in watershed simulations. Trans. ASABE 50. https://doi.org/10.13031/2013.23153.

Mtibaa, S., Hotta, N., Irie, M., 2018. Analysis of the efficacy and cost-effectiveness of best management practices for controlling sediment yield: A case study of the Joumine watershed, Tunisia. Sci. Total Environ. 616–617, 1–16. https://doi.org/10.1016/j.scitotenv.2017.10.290.

Nash, J.E., Sutcliffe, J.V., 1970. River flow forecasting through conceptual models part I — A discussion of principles. J. Hydrol. 10 (3), 282–290. https://doi.org/10.1016/0022-1694(70)90255-6.

Neitsch, S., Arnold Jeff Kiniry, J., Williams, J.R., 2011. Soil and water asessment tool theoritical documentation: Version 2009, Texas Water Resources Institute technical report No. 406. Texas Water Resources Institute, Texas A&M University, Texas. ResearchGate. https://www.researchgate.net/publication/306205252_Soil_and_water_asessment_tool_theoritical_documentation_version_2009_Texas_Water_Resources_Institute_technical_report_No_406_Texas_Water_Resources_Institute_Texas_AM_University_Texas.

Nerantzaki, S.D., Giannakis, G.V., Efstathiou, D., Nikolaidis, N.P., Sibetheros, I.A., Karatzas, G.P., Zacharias, I., 2015. Modeling suspended sediment transport and assessing the impacts of climate change in a karstic Mediterranean watershed. Sci. Total Environ. 538, 288–297. https://doi.org/10.1016/j.scitotenv.2015.07.092.

Nguyen, M.D., Baez-Villanueva, O.M., Bui, D.D., Nguyen, P.T., Ribbe, L., 2020. Harmonization of Landsat and Sentinel 2 for crop monitoring in drought prone areas: case studies of Ninh Thuan (Vietnam) and Bekaa (Lebanon). Remote Sens 12 (2). https://doi.org/10.3390/rs12020281. Article 2.

Osadchiev, A., Korshenko, E., 2017. Small river plumes off the northeastern coast of the Black Sea under average climatic and flooding discharge conditions. Ocean Sci. 13 (3), 465–482. https://doi.org/10.5194/os-13-465-2017.

Panagopoulos, Y., Makropoulos, C., Baltas, E., Mimikou, M., 2011. SWAT parameterization for the identification of critical diffuse pollution source areas under data limitations. Ecol. Model. 222 (19), 3500–3512. https://doi.org/10.1016/j.ecolmodel.2011.08.008.

Papatheodoulou, A., Tzoraki, O., Panagos, P., Taylor, H., Ebdon, J., Papageorgiou, G., Pissarides, N., Antoniou, K., Christofi, G., Dorlfinger, G., Symons, N., 2013. Simulation of daily discharge using the distributed model SWAT as a catchment management tool: Limnatis River case study. In: https://www.spiedigitallibrary.org/conference-proceedings-of-spie/8795/1/Simulation-of-daily-discharge-using-the-distributed-model-SWAT-as/10.1117/12.2035066.short.

Petrosillo, I., Scardia Scardia, A.M., Ungaro, N., Specchiulli, A., Fanelli, G., Centoducati, G., De Serio, F., Carlucci, R., Valente, D., Barbone, E., Pini, A., Giannuzzi, C.G., Scirocco, T., Lovello, E.M., Deflorio, M., Lillo, A.O., De Padova, D., Papa, L., Goffredo, E., Mossa, M., 2023. Towards sustainable marine spatial planning of aquaculture. Ecol. Indic. 154, 110542. https://doi.org/10.1016/j.ecolind.2023.110542.

Petus, C., Collier, C., Devlin, M., Rasheed, M., McKenna, S., 2014. Using MODIS data for understanding changes in seagrass meadow health: A case study in the great barrier reef (Australia). Mar. Environ. Res. 98, 68–85. https://doi.org/10.1016/j.marenvres.2014.03.006.

Pisinaras, V., Kamidis, N., Koutrakis, E., Hatzigiannakis, E., Panagopoulos, A., 2019. Simulating nutrient loads in an intensively cultivated Mediterranean watershed under current and projected climate conditions. https://doi.org/10.30955/gnc2019.00729.

Pulighe, G., Bonati, G., Colangeli, M., Traverso, L., Lupia, F., Altobelli, F., Dalla Marta, A., Napoli, M., 2020. Predicting streamflow and nutrient loadings in a semi-

arid Mediterranean watershed with ephemeral streams using the SWAT model. Agronomy 10 (1). https://doi.org/10.3390/agronomy10010002. Article 1.
Reid, A.J., Carlson, A.K., Creed, I.F., Eliason, E.J., Gell, P.A., Johnson, P.T.J., Kidd, K.A., MacCormack, T.J., Olden, J.D., Ormerod, S.J., Smol, J.P., Taylor, W.W., Tockner, K., Vermaire, J.C., Dudgeon, D., Cooke, S.J., 2019. Emerging threats and persistent conservation challenges for freshwater biodiversity. Biol. Rev. Camb. Philos. Soc. 94 (3), 849–873. https://doi.org/10.1111/brv.12480.
Ricci, G., Faouzi, Z., D'Ambrosio, E., De Girolamo, A., Parete, G., Debieche, T.-H., Gentile, F., 2022. Evaluating flow regime alterations due to point sources in intermittent rivers: A modelling approach. Journal of Agricultural Engineering 53. https://doi.org/10.4081/jae.2022.1333.
Ricci, G.F., Centanni, M., DeGirolamo, A.M., Gentile, F., 2023. Modelling daily streamflow in a temporary karst river system: comparing three approaches using the SWAT model. Hydrol. Sci. J. 68 (3), 462–473. https://doi.org/10.1080/02626667.2023.2174027.
Rosa, A., Cardoso, C., Vieira, R., Faria, R., Oliveira, A.R., Navarro, G., Caldeira, R.M.A., 2022. Frontiers | Impact of Flash Flood Events on the Coastal Waters Around Madeira Island: The "Land Mass Effect" https://doi.org/10.3389/fmars.2021.749638/full.
Salcedo-Castro, J., Olita, A., Saavedra, F., Saldías, G., Cruz-Gómez, R., Martínez, C.D., 2023. Modeling the interannual variability in Maipo and Rapel river plumes off Central Chile. Ocean Science 19, 1687–1703. https://doi.org/10.5194/os-19-1687-2023.
Salim Aoubid, H., Opp, C., 2023. Nitrogen and phosphorus discharge loads assessment using the SWAT model: A case study of the Shatt Al-Arab River basin. Appl. Sci. 13 (14), 8376. https://doi.org/10.3390/app13148376.
Sauvage, C., Lebeaupin Brossier, C., Ducrocq, V., Bouin, M.-N., Vincendon, B., Verdecchia, M., Taupier-Letage, I., Orain, F., 2018. Impact of the representation of the freshwater river input in the Western Mediterranean Sea. Ocean Model. 131, 115–131. https://doi.org/10.1016/j.ocemod.2018.09.005.
Schaeffer, B.A., Conmy Robyn, N., Duffy, Allyn E., Aukamp, Jessica, Yates, Diane F., Craven, G., 2015. Northern Gulf of Mexico estuarine coloured dissolved organic matter derived from MODIS data. Int. J. Remote Sens. 36 (8), 2219–2237. https://doi.org/10.1080/01431161.2015.1035408.
Skoulikidis, N.T., Sabater, S., Datry, T., Morais, M.M., Buffagni, A., Dörflinger, G., Zogaris, S., Del Mar Sánchez-Montoya, M., Bonada, N., Kalogianni, E., Rosado, J., Vardakas, L., De Girolamo, A.M., Tockner, K., 2017. Non-perennial Mediterranean rivers in Europe: status, pressures, and challenges for research and management. Sci. Total Environ. 577, 1–18. https://doi.org/10.1016/j.scitotenv.2016.10.147.
Soil Conservation Service (SCS), 1972. National Engineering Handbook, Section 4: Hydrology. Department of Agriculture.
Spicer, P., Cole, K.L., Huguenard, K., MacDonald, D.G., Whitney, M.M., 2021. The Effect of Bottom-Generated Tidal Mixing on Tidally Pulsed River Plumes. https://doi.org/10.1175/JPO-D-20-0228.1.
Steffen, W., Richardson, K., Rockström, J., Schellnhuber, H.J., Dube, O.P., Dutreuil, S., Lenton, T.M., Lubchenco, J., 2020. The emergence and evolution of Earth system science. Nature Reviews Earth & Environment 1 (1), 54–63. https://doi.org/10.1038/s43017-019-0005-6.
Strauss, P., Leone, A., Ripa, M.N., Turpin, N., Lescot, J.-M., Laplana, R., 2007. Using critical source areas for targeting cost-effective best management practices to mitigate phosphorus and sediment transfer at the watershed scale. Soil Use Manage. 23 (s1), 144–153. https://doi.org/10.1111/j.1475-2743.2007.00118.x.
Tavora, J., Salama, M.S., Penning de Vries, M., Mannaerts, C.M., van der Wal, D., 2023. Detecting the effects of extreme events on estuarine suspended particulate matter using satellite remote sensing (Scheldt estuary): Challenges and Opportunities. Remote Sensing 15 (3). https://doi.org/10.3390/rs15030670. Article 3.
Tramblay, Y., Rutkowska, Agnieszka, Sauquet, Eric, Sefton, Catherine, Laaha, Gregor, Osuch, Marzena, Albuquerque, Teresa, Alves, Maria Helena, Banasik, Kazimierz, Aurelien, Beaufort, Brocca, Luca, Camici, Stefania, Csabai, Zoltán, Dakhlaoui, Hamouda, DeGirolamo, Anna Maria, Dörflinger, Gerald, Gallart, Francesc, Gauster, Tobias, Hanich, Lahoucine, Datry, T., 2021a. Trends in flow intermittence for European rivers. Hydrol. Sci. J. 66 (1), 37–49. https://doi.org/10.1080/02626667.2020.1849708.
Tramblay, Y., Villarini, G., El Khalki, E.M., Gründemann, G., Hughes, D., 2021b. Evaluation of the drivers responsible for flooding in Africa. Water Resour. Res. 57 (6), e2021WR029595. https://doi.org/10.1029/2021WR029595.
Tramblay, Y., Arnaud, P., Artigue, G., Lang, M., Paquet, E., Neppel, L., Sauquet, E., 2023. HESS - changes in Mediterranean flood processes and seasonality. https://hess.copernicus.org/articles/27/2973/2023/.
Trinchera, G., Blonda, M., Gramegna, D., Ungaro, N., Lacarbonara, M., Cunsolo, S., Renna, R., 2015. Approfondimento tecnico-scientifico sulle interazioni tra il sistema ambientale ed i flussi di contaminanti da fonti primarie e secondarie nel Mar Piccolo di Taranto.
Vanhellemont, Q., Ruddick, K., 2014. Turbid wakes associated with offshore wind turbines observed with Landsat 8. Remote Sens. Environ. 145, 105–115. https://doi.org/10.1016/j.rse.2014.01.009.
Vanhellmont, Q., Ruddick, K., 2016. Acolite for Sentinel-2: Aquatic Applications of MSI Imagery, vol. 740. Living Planet Symposium, p. 55.
Verheijen, F.G.A., Jones, R.J.A., Rickson, R.J., Smith, C.J., 2009. Tolerable versus actual soil erosion rates in Europe. Earth Sci. Rev. 94 (1–4), 23–38. https://doi.org/10.1016/j.earscirev.2009.02.003.
Vizzari, M., 2022. PlanetScope, Sentinel-2, and Sentinel-1 data integration for object-based land cover classification in Google Earth Engine. Remote Sens 14 (11). https://doi.org/10.3390/rs14112628. Article 11.
Vörösmarty, C.J., McIntyre, P.B., Gessner, M.O., Dudgeon, D., Prusevich, A., Green, P., Glidden, S., Bunn, S.E., Sullivan, C.A., Liermann, C.R., Davies, P.M., 2010. Global threats to human water security and river biodiversity. Nature 467 (7315), 555–561. https://doi.org/10.1038/nature09440.
Williams, J.R., 1975. Sediment routing for agricultural watersheds. JAWRA Journal of the American Water Resources Association 11 (5), 965–974. https://doi.org/10.1111/j.1752-1688.1975.tb01817.x.
Wohl, E., Kramer, N., Ruiz-Villanueva, V., Scott, D.N., Comiti, F., Gurnell, A.M., Piegay, H., Lininger, K.B., Jaeger, K.L., Walters, D.M., Fausch, K.D., 2019. The natural wood regime in Rivers. BioScience 69 (4), 259–273. https://doi.org/10.1093/biosci/biz013.
Yang, S., Paik, K., McGrath, G.S., Urich, C., Krueger, E., Kumar, P., Rao, P.S.C., 2017. Functional topology of evolving urban drainage networks. Water Resour. Res. 53 (11), 8966–8979. https://doi.org/10.1002/2017WR021555.
Zablan, C., Blanco, A., Primavera-Tirol, Y., Nadaoka, K., 2023. Development of google earth engine application for spatiotemporal analysis of turbidity in batan estuary, aklan through the harmonization of landsat and sentinel-2 imagery. The International Archives of the Photogrammetry Remote Sensing and Spatial Information Sciences XLVIII-1 (W2–2023), 1965–1971. https://doi.org/10.5194/isprs-archives-XLVIII-1-W2-2023-1965-2023.
Zuffianò, L.E., Basso, A., Casarano, D., Dragone, V., Limoni, P.P., Romanazzi, A., Santaloia, F., Polemio, M., 2016. Coastal hydrogeological system of Mar piccolo (Taranto, Italy). Environ. Sci. Pollut. Res. 23 (13), 12502–12514. https://doi.org/10.1007/s11356-015-4932-6.